Structural and collective properties of two-dimensional Yukawa liquids

2003 J. Phys. A: Math. Gen. 36 6273

(http://iopscience.iop.org/0305-4470/36/22/358)

INSTITUTE OF PHYSICS PUBLISHING JOURNAL OF PHYSICS A: MATHEMATICAL AND GENERAL

J. Phys. A: Math. Gen. **36** (2003) 6273–6280 PII: S0305-4470(03)55652-9

Structural and collective properties of two-dimensional Yukawa liquids

Michael S Murillo and Dirk O Gericke

Theoretical Division, Los Alamos National Laboratory, Los Alamos, NM 87545, USA

E-mail: murillo@lanl.gov

Received 29 October 2002, in final form 4 December 2002
Published 22 May 2003
Online at stacks.iop.org/JPhysA/36/6273

Abstract

The radial distribution function of two-dimensional Yukawa systems has been computed with the hypernetted chain equations and compared with molecular dynamics simulations. A comparison is also made with similar quantities in three-dimensional systems. The importance of the bridge function in two dimensions is illustrated. Collective behaviour is described in terms of the dynamic structure factor $S(q, \omega)$; inclusion of the local field correction $G(q, \omega)$ incorporates physics beyond the random phase approximation. Simulation results are compared with renormalized mean-field approximations $G(q, \omega) \approx G(q, 0)$ and $G(q, \omega) \approx G(q, \infty)$. These approximations fail to capture details of the spectrum.

PACS numbers: 52.27.Gr, 52.27.Lw, 62.22.+m

1. Introduction

A variety of strongly coupled Coulomb systems confined to a single layer exist; examples are electrons trapped on helium surfaces [1] or within semiconductor heterojunctions [2], and monolayer dusty plasmas [3]. Structural properties of the pure Coulomb case have been considered previously [4], as have the collective properties [5]. Since the statistical mechanics of many-body systems can depend on the dimensionality of the system, it is of interest to explore the properties of two-dimensional (2D) Yukawa systems, whose three-dimensional (3D) counterparts have recently received considerable attention. For example, structural properties [6] and the phase diagram [7] have been considered, as have the transport coefficients of diffusion [8] and viscosity [9]. The collective properties, including both longitudinal and transverse modes, have been elucidated using a variety of techniques [10–13]. Here we focus on the radial distribution function and the dynamic structure factor of 2D Yukawa systems and draw comparisons to 3D systems.

For screened systems we consider N particles confined to an area A with a real density $n = N/A$. In two dimensions we define the temperature as $k_B T = \frac{m}{2}\langle v_x^2 + v_y^2\rangle \equiv \beta^{-1}$. The pair interaction between particles is taken to be

$$\beta v(r) = \frac{\Gamma}{r}\exp(-\kappa r) \qquad u(q) \equiv \beta n v(q) = \frac{2\Gamma}{\sqrt{\kappa^2 + q^2}}$$

in real and Fourier space, respectively. Lengths are in units of the ion-circle radius $a = (\pi n)^{-1/2}$. The dimensionless coupling parameter Γ and screening parameter κ are defined as

$$\Gamma = \frac{\beta Q^2}{a} \qquad \kappa = \frac{a}{\lambda}. \tag{1}$$

The physical screening length is λ and Q is the average charge. For typical dust grains, Q is negative and of order $Q \sim -10^{3-4}|e|$ and the background plasma screens the grains, which is characterized by λ [14].

The radial distribution function $g(r)$ is computed both with integral equations and with molecular dynamics simulation and the results are compared for 2D and 3D systems in section 2. This quantity forms the basic ingredient for describing the effects of strong coupling on the density fluctuation spectrum $S(q, \omega)$, which is considered in section 3.

2. Structural properties

The thermodynamic properties of many-body systems describable in terms of a pair potential can be computed from knowledge of the radial distribution function $g(r)$ [15]. The formally exact integral equations for $g(r)$ are

$$\begin{aligned} \ln g(r) &= -\beta v(r) + h(r) - c(r) + B(r) \\ h(r) &= c(r) + \frac{1}{\pi}\int \mathrm{d}^2 r'\, h(|r - r'|)c(r') \\ g(r) &= h(r) + 1. \end{aligned} \tag{2}$$

Equations (2) are adapted to the two-dimensional Yukawa case in the hypernetted chain (HNC) approximation, in which the bridge function is neglected ($B(r) = 0$); this adaptation occurs in the Fourier transform of the middle equation, which now involves cylindrical, rather than spherical, Bessel functions [16]. The static structure factor $S(q)$ is an important related quantity, and is related to $g(r)$ through a Fourier transform relation

$$S(q) = 1 + \frac{1}{\pi}\int \mathrm{d}^2 r [g(r) - 1]\,\mathrm{e}^{-\mathrm{i}\mathbf{q}\cdot\mathbf{r}}. \tag{3}$$

This quantity will play an important role in describing the spectrum of density fluctuations.

We have compared solutions of equations (2) to molecular dynamics results and find good agreement for weak to moderate coupling. A typical result for strong coupling conditions $\Gamma = 100$ and $\kappa = 2$ is shown in figure 1 for both 2D and 3D. These parameters are chosen because they both correspond to possible conditions in a dusty plasma and to illustrate the physics in an intermediate regime with neither very weak nor very strong coupling. (In 3D the Yukawa parameters are defined analogously to equations (1) [7].) These parameters correspond to an effective coupling[1] of $\Gamma_{\mathrm{eff}} \equiv \Gamma \mathrm{e}^{-\kappa} \approx 13.5$. It is clear that the peak structure is more pronounced in 2D (red curves) than in 3D (blue curves) for the same Yukawa parameters,

[1] This definition of effective coupling is used only to illustrate that the large bare coupling of $\Gamma = 100$ is reduced by the effects of screening, as characterized by $\kappa = 2$; in fact, there is no unique definition of the effective coupling. For a discussion of effective coupling parameters see, for example, the first citation of [9].

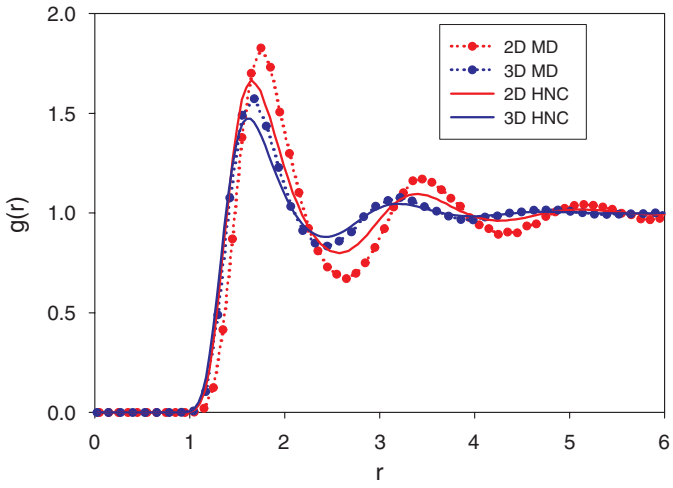

Figure 1. Radial distribution functions $g(r)$ for Yukawa parameters $\Gamma = 100$ and $\kappa = 2$. Comparison is made between 2D (red curves) and 3D (blue curves) systems; both HNC and MD results are shown.

and that the corresponding 2D HNC calculation is less accurate. Note that, although the HNC underestimates the first peak in 3D, the remaining peaks are fairly well described, in contrast to the 2D result. This point is obviously related to the fact that the one-component plasma (OCP) melting transition for 2D systems [17] $\Gamma_m^{2D} \approx 130$ tends to occur at lower values of Γ than for 3D systems [7] $\Gamma_m^{3D} \approx 170$.

3. Dynamical properties

Given knowledge of the structural properties, we can now compute collective properties. The collective modes are described generally in terms of the dynamic structure factor (DSF) and current autocorrelation functions. After a general discussion, the simplest approximation, the random phase approximation (RPA), is presented. Then, the local field correction in two static approximations is introduced.

3.1. General definitions

The dynamics of the 2D Yukawa system can be characterized by the autocorrelation function of density fluctuations $\delta n(q,t)$ in mode q, namely

$$S(q,\omega) = \frac{1}{N\omega_0}\int_{-\infty}^{\infty} \mathrm{d}t\,\langle \delta n(q,t)\delta n(-q,0)\rangle\, \mathrm{e}^{\mathrm{i}\omega t}. \tag{4}$$

Here time and length quantities are written in terms of the frequency $\omega_0 = \sqrt{\frac{2\pi n Q^2}{am}}$ and length a, respectively. This quantity, the DSF, can be related to the density response function $\chi(q,\omega)$ through the fluctuation–dissipation theorem

$$S(q,\omega) = -\frac{2}{\beta n\omega}\,\mathrm{Im}[\chi(q,\omega)]. \tag{5}$$

An important sum rule relates the DSF to the static structure factor

$$\langle \omega^0 \rangle = \int_{-\infty}^{\infty} \frac{\mathrm{d}\omega}{2\pi} S(q,\omega) = S(q). \tag{6}$$

This relation provides a constraint on the dynamics through the known static properties of equation (3). There are two other 'basic' sum rules that further constrain approximate dynamical theories. These are the f-sum rule,

$$\langle\omega^2\rangle = \int_{-\infty}^{\infty} \frac{\mathrm{d}\omega}{2\pi}\omega^2 S(q,\omega) = \frac{q^2}{2\Gamma} \tag{7}$$

and the fourth-moment sum rule

$$\begin{aligned}\langle\omega^4\rangle &= \int_{-\infty}^{\infty} \frac{\mathrm{d}\omega}{2\pi}\omega^4 S(q,\omega) \\ &= \frac{3q^4}{(2\Gamma)^2} + \frac{q^2}{2\pi(2\Gamma)}\int \mathrm{d}^2 r\, g(r)[1-\mathrm{e}^{-\mathrm{i}qx}]\frac{\partial^2}{\partial x^2}\left(\frac{\mathrm{e}^{-\kappa r}}{r}\right).\end{aligned}$$

The importance of these sum rules is that exact static properties constrain dynamical theories; below, the sum rules will be related to the frequency response.

It is convenient to parametrize the density response function as

$$\chi(q,\omega) = \frac{\chi^{(0)}(q,\omega)}{1 - v(q)[1-G(q,\omega)]\chi^{(0)}(q,\omega)} \tag{8}$$

where $G(q,\omega)$ is the dynamic local field correction (DLFC) [18]. The ideal gas response function is given by

$$\chi^{(0)}(q,\omega) = -\beta n\left[1 + \mathrm{i}\sqrt{\pi\Gamma}\frac{\omega}{q}\mathcal{W}\left(\sqrt{\Gamma}\frac{\omega}{q}\right)\right]$$

where the function

$$\mathcal{W}(z) = \mathrm{e}^{-z^2}\mathrm{erfc}(-\mathrm{i}z)$$

is related to the complex error function [20]. Note that equation (8) is exact by definition; therefore $G(q,\omega)$ contains all physics beyond the RPA.

3.2. Random phase approximation

For weakly coupled systems, the simplest approximation to equation (8) corresponds to

$$\chi(q,\omega) = \frac{\chi^{(0)}(q,\omega)}{1 - v(q)\chi^{(0)}(q,\omega)}$$

which is the RPA (Vlasov) result, defined as $G(q,\omega) = 0$. In the limit $\omega \to \infty$ and with $\mathrm{Im}[\chi^{(0)}(q,\omega)] \approx 0$, we can find the approximate dispersion relation

$$\omega_{\mathrm{RPA}}(q) = \omega_0\frac{q}{(q^2+\kappa^2)^{1/4}} \tag{9}$$

which is acoustic in the long-wavelength limit. (Note that for the pure OCP, $\omega_{\mathrm{OCP}}(q) = \omega_0\sqrt{q}$.)

3.3. Local field corrections

It is possible to extend the applicability of the RPA result into the strong coupling regime by including the DLFC. Unfortunately, it is difficult to construct the DLFC, even approximately. Here two static forms are used that satisfy two, but different, sum rules.

As a first approximation, we will enforce the $\langle\omega^0\rangle$ and $\langle\omega^2\rangle$ sum rules. The $\langle\omega^2\rangle$ sum rule is trivially satisfied by the form of equation (8). The $\langle\omega^0\rangle$ sum rule can be enforced with

a combination of equations (5) and (6) with the Kramers–Kronig relation for $\chi(q,\omega)$ [19] to yield

$$G(q,0) = 1 - \frac{1}{u(q)}\left(\frac{1}{S(q)} - 1\right). \tag{10}$$

This approximation is referred to as the static local field correction (SLFC) approximation, and obviously treats strong coupling behaviour in a low-frequency approximation. The SLFC is equivalent to replacing the pair interaction by the direct correlation function, as $u(q) \to -c(q)/\pi$.

If the sum rules $\langle\omega^2\rangle$ and $\langle\omega^4\rangle$ are used, a second approximation is

$$G(q,\infty) = -\frac{1}{2\pi q}\int \mathrm{d}^2 r\, h(r)[1 - \mathrm{e}^{-\mathrm{i}qx}]\frac{\partial^2}{\partial x^2}\left(\frac{\mathrm{e}^{-\kappa r}}{r}\right) \tag{11}$$

which treats strong coupling behaviour in a high-frequency approximation. We will refer to this result as the high-frequency local field correction (HFLFC).

It is important to point out that equations (10) and (11) are renormalized mean field results in the sense that the pair interaction is replaced by an effective interaction that obeys specific sum rules (to the accuracy that $g(r)$ is known) but the *dynamics* is still governed by the RPA; therefore, the only damping mechanism included is the Landau damping. This can be seen by noting that both the SLFC and the HFLFC approximations can be obtained from the Vlasov equation with static effective interactions of the form $v(q)\,[1 - G(q,0)]$ and $v(q)\,[1 - G(q,\infty)]$, respectively; the underlying kinetic equation is not modified, but the pair interaction is. An extension of the RPA dynamics requires a frequency-dependent DLFC $G(q,\omega)$. Although we do not consider it here, it should be mentioned that a simple DLFC can be constructed that satisfies all three sum rules $\langle\omega^{0,2,4}\rangle$ [21].

4. Molecular dynamics simulation

Molecular dynamics (MD) simulations have been performed to assess the accuracy of equations (10) and (11) for the case $\Gamma = 100$ and $\kappa = 2$. The simulations were performed in a square cell with periodic boundary conditions; no Ewald sum was needed for the large κ value considered. To obtain the spectrum at long wavelengths, which from equation (9) also corresponds to low frequencies, simulations were performed with $N = 500$ particles for a time interval of $T = 2400\omega_0^{-1}$. To ensure accurate energy conservation, a time step of $\Delta t = 0.03\omega_0^{-1}$ was used. After an initial equilibration phase, simulations were performed in the microcanonical ensemble.

In addition to energy conservation, the accuracy of the simulation and analysis was also confirmed by checking both the f-sum rule, equation (7), and the continuity equation, which connects the density fluctuation spectrum of equation (4) to the spectrum of longitudinal current fluctuations $j(q,t) \equiv \hat{\mathbf{q}}\cdot\mathbf{j}(q,t)$ through

$$C_L(q,\omega) = \frac{1}{N}\int_{-\infty}^{\infty}\mathrm{d}t\langle j(q,t)\,j(-q,0)\rangle\,\mathrm{e}^{\mathrm{i}\omega t} = \frac{\omega^2}{q^2}S(q,\omega).$$

The f-sum rule was satisfied to within ~23% for small q and ~3% for large q; the error for small q is likely due to insufficient frequency samping near the strong peaks. The difference between $q^2C_L(q,\omega)/\omega^2$ and $S(q,\omega)$ was much less than a per cent.

5. Results

The spectrum $\omega_0 S(q,\omega)$ is shown in figure 2 for wavevectors $q = 0.159$ (red), $q = 0.476$ (green) and $q = 0.793$ (blue) from MD and the theoretical model of equation (10). The model

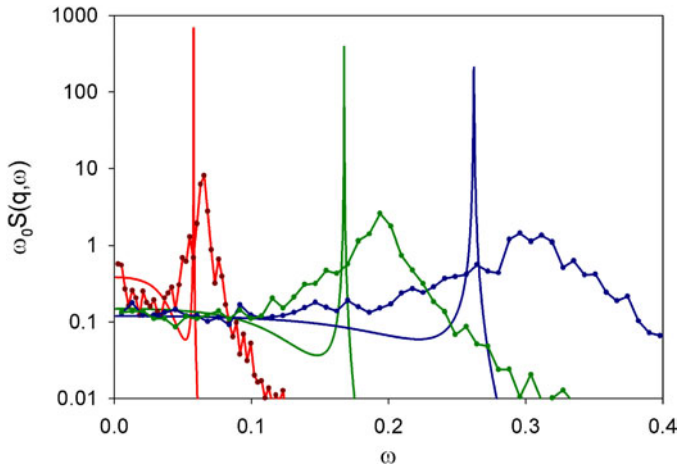

Figure 2. Dynamic structure factors computed in the approximation $G(q,\omega) \approx G(q,0)$, as compared with (2D) MD for Yukawa plasma parameters $\Gamma = 100$ and $\kappa = 2$. The wavevectors are $q = 0.159$ (red), $q = 0.476$ (green) and $q = 0.793$ (blue).

of equation (11) is not shown due to its inaccuracy—see the dispersion relation discussion below. All theoretical models greatly underestimate the width of the spectrum, which indicates an important deficit of the renormalized mean-field approach. However, the dispersion relation is predicted fairly well, as estimated by

$$\omega(q;0) = \omega_0 \frac{q\sqrt{1-G(q,0)}}{(q^2+\kappa^2)^{1/4}} \tag{12}$$

$$\omega(q;\infty) = \omega_0 \frac{q\sqrt{1-G(q,\infty)}}{(q^2+\kappa^2)^{1/4}}. \tag{13}$$

These dispersion relations are the approximate poles of equation (8), as obtained by expanding $\chi^{(0)}(q,\omega)$ at high frequency and neglecting $\mathrm{Im}[\chi^{(0)}(q,\omega)]$. The latter estimate, equation (13), can be shown to be closely related to mode dispersion in amorphous solids and liquids [22], and is sometimes referred to as the quasilocalized charge approximation [23]. Here equation (13) extends those results to the 2D Yukawa case. The dispersion relation is shown in figure 3. The dispersion relation has been obtained both with the simple estimates of equations (12) and (13), and from the peak of $S(q,\omega)$ from equation (5) as evaluated in the SLFC approximation. The outcome that equation (12) yields superior results suggests that caging is relatively weak for this particular case. Note that the estimate of equation (12) predicts frequencies below the actual peak frequencies of $S(q,\omega)$. It is worth noting that the estimates of equations (12) and (13) will yield slightly lower frequencies if a bridge function $B(r)$ is included in calculation of equations (2). Currently the 2D Yukawa bridge function is not known, although it is approximately known for 3D Yukawa systems [6].

The transverse current autocorrelation function

$$C_T(q,\omega) = \frac{1}{N}\int_{-\infty}^{\infty} \mathrm{d}t \langle j_T(q,t)\, j_T(-q,0)\rangle \, \mathrm{e}^{\mathrm{i}\omega t} \tag{14}$$

where $j_T(q,t)$ is transverse to q, was also computed by MD. Only the $\omega = 0$ diffusive mode was observed, except at the shortest wavelength $q = 0.793$ where a propagating mode appeared. A single square is shown in figure 3; this behaviour is qualitatively consistent with

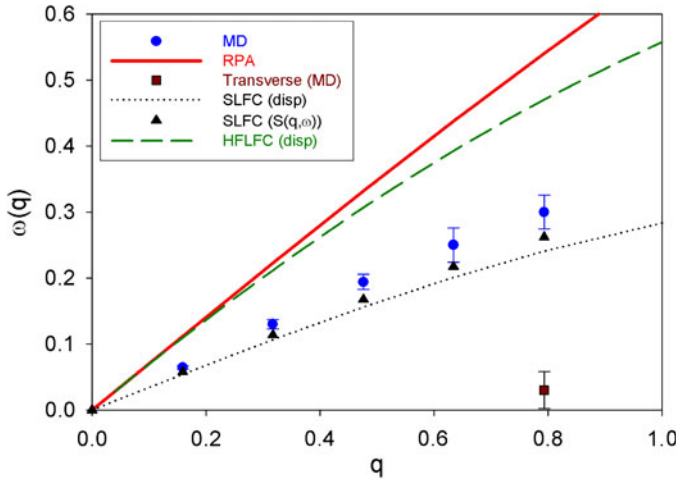

Figure 3. Dispersion relation for the longitudinal mode for $\Gamma = 100$ and $\kappa = 2$. Blue points are (2D) MD results with error bars indicating the width at half the peak value. The curves correspond to the theoretical predictions: solid red is the RPA dispersion relation; dashed green is the HFLFC dispersion relation, dotted black is the SLFC dispersion relation; black triangles are the peaks of $S(q, \omega)$ in the SLFC approximation and the dark red square is the appearance of the transverse mode.

predictions made for 3D systems [11]. This result suggests that, for the specific case being considered, all other wavevectors $q < 0.793$ are in the hydrodynamic limit.

6. Conclusion

We have shown that the HNC integral equations approximately describe the structure of the 2D Yukawa fluid, although a bridge function $B(r)$ should be used for fluids near freezing. For a consistent set of Yukawa parameters we have found that the 2D fluid has more pronounced peaks in the radial distribution function than the corresponding 3D fluid.

We have also calculated the spectrum of density and current fluctuations in two renormalized mean-field approximations, and these results have been compared with MD results. We find that, for the case $\Gamma = 100$ and $\kappa = 2$, the theoretical models cannot accurately predict the spectrum, although the dispersion is fairly well described by the SLFC. The dispersion relation has been shown to be somewhat sensitive to using the peaks of $S(q, \omega)$ versus simple estimates. The error in the width is a consequence of neglecting damping in the mean-field models, which only treat Landau damping. Extensions of this mean-field approach can be made by introducing transport information [10, 11]; however, transport properties (e.g., viscosity) of 2D Yukawa systems are not yet known.

References

[1] Leiderer P 1992 *J. Low Temp. Phys.* **87** 247
[2] Williams F I B *et al* 1992 *Surf. Sci.* **263** 23
[3] Juan W T and Lin I 1998 *Phys. Rev. Lett.* **80** 3073
[4] Totsuji H 1978 *Phys. Rev.* A **17** 399
[5] Totsuji H and Kakeya H 1980 *Phys. Rev.* A **22** 1220
Moudgil R K and Ahluwalia P K 1996 *Phys. Rev.* B **54** 8809

[6] Daughton W, Murillo M S and Thode L 2000 *Phys. Rev.* E **61** 2129
[7] Hamaguchi S, Farouki R T and Dubin D H E 1997 *Phys. Rev.* E **56** 4671
[8] Ohta H and Hamaguchi S 2000 *Phys. Plasmas* **7** 4506
Rosenfeld Y 2000 *Phys. Rev.* E **62** 7524
[9] Murillo M S 2000 *Phys. Rev.* E **62** 4115
Sanbonmatsu K Y and Murillo M S 2001 *Phys. Rev. Lett.* **86** 1215
Saigo T and Hamaguchi S 2002 *Phys. Plasmas* **9** 1210
Salin G and Caillol J M 2002 *Phys. Rev. Lett.* **8806** 5002
[10] Murillo M S 2000 *Phys. Plasmas* **7** 33
[11] Murillo M S 2000 *Phys. Rev. Lett.* **85** 2514
[12] Ohta H and Hamaguchi S 2000 *Phys. Rev. Lett.* **84** 6026
[13] Kalman G, Rosenberg M and DeWitt H E 2000 *Phys. Rev. Lett.* **84** 6030
[14] Lemons D S, Murillo M S, Daughton W and Winske D 2000 *Phys. Plasmas* **7** 2306
[15] Baus M and Hansen J-P 1980 *Phys. Rep.* **59** 2
[16] Lado F 1978 *Phys. Rev.* B **17** 2827
[17] Grimes C C and Adams G 1979 *Phys. Rev. Lett.* **42** 795
Morf R H 1979 *Phys. Rev. Lett.* **43** 931
[18] Ichimaru S 1992 *Statistical Plasma Physics, Volume I: Basic Principles* (New York: Addison-Wesley) p 71
[19] Ichimaru S 1992 *Statistical Plasma Physics, Volume I: Basic Principles* (New York: Addison-Wesley) p 64
[20] Abramowitz M and Stegun I A 1972 *Handbook of Mathematical Functions* (New York: Dover) p 295
[21] Hong J and Kim C 1991 *Phys. Rev.* A **43** 1965
[22] Hubbard J and Beeby J L 1969 *J. Phys. C: Solid State Phys.* **2** 556
[23] Golden K I and Kalman G J 2000 *Phys. Plasmas* **7** 14